Environ. Sci. Technol. **2007**, *41*, 936−941

Spatial Distributions of Copper in Microbial Biofilms by Scanning Electrochemical Microscopy

ZHIQIANG HU,[†,‡] JING JIN,[§] HÉCTOR D. ABRUÑA,[§] PAUL L. HOUSTON,[§] ANTHONY G. HAY,[∥] WILLIAM C. GHIORSE,[∥] MICHAEL L. SHULER,[⊥] GABRIELA HIDALGO,[‡] AND LEONARD W. LION*[,‡]

School of Civil and Environmental Engineering, Department of Chemistry and Chemical Biology, Department of Microbiology, School of Chemical and Biomolecular Engineering, Cornell University, Ithaca, New York 14853, and Department of Civil and Environmental Engineering, University of Missouri—Columbia, Columbia, Missouri 65211

The spatial distribution of Cu was determined in *Escherichia coli* PHL628 biofilms using a scanning electrochemical microscope (SECM) consisting of a microelectrode in conjunction with a piezoelectric micropositioning system. Aqueous labile copper species were determined using voltametric stripping after reductive deposition of Cu for 4 min on the microelectrode at −0.7 V (vs Ag/AgCl). The position of the bulk solution-biofilm interface was determined from the change in current produced by 0.4 mM hydroxymethyl ferrocene that was added as a redox indicator. After a 2 h exposure to 0.2 mM copper, Cu was located in the upper region of the biofilm with a penetration depth less than 150 μm. A one-dimensional diffusive transport model adequately described the spatial distribution of copper in the biofilm, but the Cu retardation factor in the biofilm was more than 6-fold larger than that calculated from the isotherm for Cu binding to suspensions of *E. coli* PHL628 cells. There are several possible reasons for this difference, including an increase in the amount of extracellular polymer per cell within the biofilm and/or tortuosity that might hinder Cu transport into biofilms. The SECM technique in combination with model calculations provides direct evidence in support of the concept that formation of a biofilm may confer resistance to transient spikes in the bulk solution concentration of toxic metal species by retarding metal diffusion and reducing the metal exposure of cells within the biofilm.

Introduction

Surfaces in both natural and engineered systems are typically colonized by adherent bacteria resulting in heterogeneous surface coatings (or biofilms) consisting of the attached microbial population and extracellular polymer materials of bacterial origin (*1*−*4*). In biofilms, biological, physical, and chemical processes influence one another over a broad range of time and spatial scales, resulting in complex macroscopic 3-D structures containing pores, channels, and mushroom-shaped protuberances (*3*−*6*). These structural features are generally similar in biofilms formed by single species or by naturally occurring mixed species consortia (*3*, *4*, *7*).

Biofilms are ubiquitous in nature, but the ecological advantages of forming biofilms versus planktonic growth are not well understood. Advantages associated with adherent growth are thought to include the formation of microniches that permit metabolic diversity and the opportunity that close cell-to-cell proximity confers for the transfer of genetic information (*4*, *8*). Recent advances in characterizing differential gene expression and the roles of quorum sensing molecules have improved our understanding of changes in bacteria that are associated with biofilm formation (*9*, *10*). Adherent bacteria are typically embedded within a matrix of extracellular polymeric substances (EPS) of bacterial origin. The EPS matrix includes complex mixtures of heteropolysaccharides, protein, and nucleic acids (*4*, *11*, *12*) that can provide protection from a variety of environmental stresses, such as UV radiation (*13*), desiccation (*14*), and toxins (e.g., antimicrobial agents (*15*) and heavy metals (*10*, *16*)).

Trace metals are also ubiquitous in nature, and their interactions with biofilms are of great interest. Surface complexation of metals with biofilms plays a role in controlling the phase distribution, bioavailability, and the biogeochemical cycling of many metal species in natural aquatic systems. Trace metals, in turn, affect microbial growth both as nutrients and toxins (*10*, *17*, *18*). Previous studies of biofilms and metal interactions have demonstrated that metals strongly adsorb to biofilms (*10*, *19*). In the case of biofilm exposure to copper, results obtained through scanning confocal laser microscopy (SCLM) revealed that the exterior of a *Pseudomonas aeruginosa* biofilm was dead after exposure to elevated concentrations of copper while most cells near the attachment surface were live, an indication of differential exposure to Cu as a function of position within the biofilm (*10*). Recent results by the authors using a zinc specific fluorochrome and two-photon laser scanning microscopy showed that zinc diffusion over a distance of 20 μm into *Escherichia coli* biofilms required a time scale of hours (*6*).

In this paper we describe a new technique, scanning electrochemical microscopy (SECM), for determination of the spatial distributions of metals in microbial biofilms. SECM is based on measurement of faradic current changes as a microelectrode is moved (with submicron precision) in a sample matrix (*20*). It is a viable method for noninvasive imaging of the electroactive components of surfaces at the micrometer scale and below (see recent monograph by Bard and Mirkin for additional experimental details and applications of SECM (*21*)), and it has a wide range of applications to targets of biological origin including enzymes (*29*, *30*), cells (*31*, *32*), and DNA (*33*). In this study, SECM was applied to permit metal analysis of thicker biofilms than are amenable to observation with laser scanning microscopy. Distribution of dissolved copper (Cu^{2+} and electrochemically labile complexes) was evaluated in *Escherichia coli* biofilms. In addition, a diffusive transport model was fit to the observed metal distribution and used to estimate a retardation coefficient for Cu transport.

Materials and Methods

Bacterial Strains and Media. The test bacterium used in these experiments was *Escherichia coli* PHL628. *E. coli* PHL628

* Corresponding author phone: (607)255-7571; fax: (607)255-9004; e-mail: LWL3@cornell.edu.

† Current address: Department of Civil and Environmental Engineering, University of Missouri—Columbia.

‡ School of Civil and Environmental Engineering.

§ Department of Chemistry and Chemical Biology.

∥ Department of Microbiology.

⊥ School of Chemical and Biomolecular Engineering.

10.1021/es061293k CCC: $37.00
Published on Web 12/20/2006

is a K12 MG1655 derivative that forms biofilms as a result of overexpression of curli (*22*). The *E. coli* strain was selected for convenience to provide a reproducible biofilm matrix for use in methods development. The strain was first grown in a modified minimum mineral salts (MMS) medium (*17*), which contained per liter: 3 g $CaCl_2 \cdot 2H_2O$, 3.5 g $MgSO_4 \cdot 7H_2O$, 12 g $(NH_4)_2SO_4$, 1.5 g KNO_3, 0.084 g $NaHCO_3$, 5 g KH_2PO_4, 1.7 g sodium pyruvate, and 20 mmol 4-(2-hydroxyethyl)-1-piperazineethanesulfonic acid (HEPES) with pH adjusted to 7.0. A complete Luria−Bertani (LB) medium containing, per liter, 10 g tryptone, 5 g yeast, and 10 g NaCl was used as a matter of expedience since it allowed us to develop a very thick biofilm sample for SECM analysis with a short period of time (in a few days). All media were sterilized by autoclaving at 121 °C before use.

Biofilms. The methods used for biofilm cultivation are described in detail by Hu et al. (*6*). Briefly, *E. coli* cells were grown overnight in MMS in Erlenmeyer culture flasks at 37 °C. Aliquots (0.5 mL) of an overnight culture were added in microwell dishes with 0.17 mm glass coverslips at the bottom (MatTek, Ashland, MA), diluted 6-fold with the same medium, and incubated on a mechanical shaker (50 rpm) at 30 °C. The 30 °C temperature facilitated overexpression of curli and biofilm formation.

Inoculated microwell dishes were kept overnight before a flow containing LB medium was initiated. The LB medium was delivered with a Masterflex peristaltic pump (Cole-Parmer, Vernon Hills, IL) and dripped onto the glass coverslips in microwell dishes at a constant flow rate of 0.08 mL/min at 30 °C. The *E. coli* biofilms were harvested after 4 days growth in the continuous feed system with LB.

Copper Adsorption to Biofilms. Residual LB medium was decanted from the *E. coli* biofilms, and they were rinsed twice with deionized H_2O. A 4 mL volume of 0.2 mM $Cu(NO_3)_2$ solution (pH = 7) containing 20 mM HEPES and 100 mM $NaNO_3$ (as electrolyte) was added to the microwell dish containing biofilms. At predetermined intervals (0.5−2.5 h), the residual copper concentrations in the bulk aqueous solution were measured by cyclic voltammetry using a scanning electrochemical microscope as described below. The amount of Cu sorbed to biofilms was calculated from the difference between the initial and the measured dissolved Cu concentrations. A control experiment in the absence of biofilms was also conducted to correct for wall loss of Cu over time.

Copper Sorption to Planktonic Bacteria. Cu sorption isotherms were obtained for overnight cultures of *E. coli* PHL628 cells in early stationary phase and used to estimate the retardation factor (R_f) for diffusive transport of Cu into biofilms. The cultures were adjusted to pH 7.0 before use. Aliquots of Cu stock solution were added to cell suspensions to achieve metal doses from 0 to 1.5 mM, and sample pH was maintained at pH 7.0 through the addition of 0.1 N NaOH. The samples were incubated at room temperature (25 °C) on a shaker at 300 rpm for 1 h (based on the results of a previous kinetic study (*6*)) before they were withdrawn and centrifuged at 20000 × *g* for 30 min. Dissolved Cu concentrations were determined from the supernatants using an AAanalyst 100 atomic absorption spectrophotometer (Perkin-Elmer, Norwalk, CT), and the amount of sorbed Cu was calculated by difference from the total added Cu to determine Cu adsorption isotherms. The slope of the linear region of the isotherm, K_d, was used to estimate the Cu retardation factor as follows

$$R_f = 1 + \left(\frac{X_B}{\phi}\right)K_d \quad (1)$$

where X_B and ϕ are bulk cell density (g/L) and porosity, respectively, in *E. coli* biofilms.

All glassware and plastic tubes were acid washed prior to use in experiments. Measurements were performed in duplicate unless otherwise stated. Concentrations of planktonic and biofilm biomass were measured as chemical oxygen demand (COD) according to standard methods (*23*) using commercially available reagents (HACH COD vials, Loveland, CO). COD is a common measure of organic carbon (the biofilm in this case), expressed in terms of the amount of oxygen required for oxidation to carbon dioxide.

SECM Measurements. Copper concentrations in bulk solutions and biofilms were measured with a scanning electrochemical microscope (SECM) (CH Instruments, Austin, TX). The microscope is composed of a piezoelectric based microposition controller (Inchworm motors, Burleigh Instruments), a potentiostat to maintain constant potential of the working electrode, and a 25 μm diameter microelectrode that produced a faradic current signal from electrolysis of solution species. The SECM assembly was interfaced with a personal computer for control and data acquisition (a schematic of the apparatus assembly is shown in Figure S1, Supporting Information).

The Pt working microelectrode was prepared as described by Pendley and Abruña with some modifications (24). Briefly, a mechanical puller was used to produce an annealed soft-glass capillary that at one end has the same order of size (confirmed under microscope) as the micrometer-sized Pt wire. A 1−1.5 cm long Pt wire with diameter of 25 μm was inserted into the soft-glass capillary. The Pt wire and glass capillary were then fused in a small furnace such that the glass coated the wire. The tip was carefully polished with diamond pastes so that the glass insulator formed a truncated cone around the disk shaped Pt electrode. An electrical contact between the Pt and a wire connected to the SECM was established using silver epoxy glue. The Pt microelectrode was electrochemically cleaned in 0.1 M H_2SO_4 solution before a series of measurements was performed.

E. coli biofilms were washed (×2) with deionized water before they were exposed to 0.2 mM Cu for 2 h. The exposed biofilms were rinsed (×2) with deionized water and were then submerged into a solution containing 10 mM HEPES, 50 mM $NaNO_3$, and 0.4 mM hydroxymethyl ferrocene [$Fe(C_5H_5)(C_5H_4)CH_2OH$] as a redox indicator. The steady-state current of hydroxymethyl ferrocene was continuously recorded at constant potential of 0.5 V as the microelectrode tip approached the biofilm. The biofilm−bulk solution interface was identified by a sharp drop (>50%) in current (*20*, *21*), which is attributed to impaired diffusion of hydroxymethyl ferrocene to the microelectrode caused by close approach to the biofilm surface (see Discussion section). This magnitude of drop typically occurred over a short distance (≈25 μm) in proximity to from the biofilm surface. Since the aqueous copper concentrations within biofilms were very low, the microelectrode tip was held at −0.7 V for 4 min to preconcentrate aqueous copper species onto the tip before a voltametric measurement was initiated. The preconcentration step at −0.7 V was carefully selected because of the observation that significant overpotential must be applied to make the reaction proceed in a reasonable time (i.e., detectable Cu concentrations after 4 min preconcentration). A series of such measurements were performed at the same lateral position as the microelectrode tip penetrated perpendicularly into the biofilms at a time interval of 6−10 min between different depths into the biofilm. The Cu concentrations of duplicate measurements while holding the tip in the same place in the biofilm were within ±9.9% (data not shown). A plot of current versus potential (from −0.5 to 0.7 V, see Figure 2) was recorded at a scan rate of 50 mV/s (minimum of 3 scans) using the microelectrode, a Ag/AgCl reference electrode, and a counter electrode in the unstirred bulk solution. Calibration curves with and without

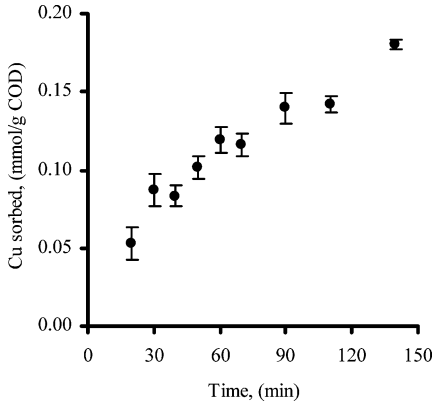

FIGURE 1. Kinetics of Cu adsorption to *E. coli* biofilms ($X = 791 \pm 16$ mg COD/L) after the addition of 0.2 mM Cu.

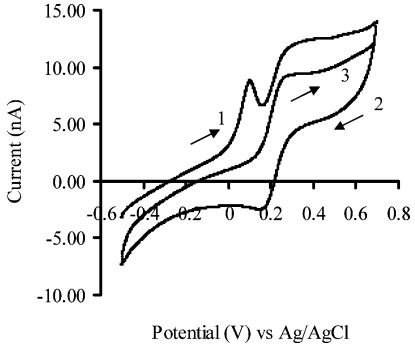

FIGURE 2. Cyclic voltammograms at a scan rate of 50 mV/s using a Pt microelectrode in a copper-treated biofilm that was exposed to 0.4 mM hydroxymethyl ferrocene solution as a redox indicator. Aqueous copper species in the biofilm were concentrated on the Pt microelectrode for 4 min at −0.7 V before an electrochemical scan was initiated. For the anodic scan (line 1) the peak corresponding to Cu oxidation can be seen at 0.1 V. No Cu peak was observed on the subsequent anodic scan (line 3), which was performed without the 4 min predeposition of Cu.

the 4 min preconcentration step were established between peak area (coulombs) and bulk copper concentrations for analysis of experimental data. Microelectrodes are commonly calibrated in bulk solution (*34*−*36*) although calibration has also been performed in a 0.5% agar gel containing the species of interest (*37*). We tested for differences in electrode response in the bulk solution versus the biofilm by equilibrating a biofilm with 0.08 mM Cu over 2 days during which the Cu solution was replaced six times. After this equilibration it is likely that the Cu concentration in the fluid in the upper portion of the biofilm matrix would be the same as that in the bulk aqueous phase. The measured Cu signal in the biofilm pore fluid was 11.8% of that in the bulk solution, and the difference was assumed to result from the combined effects of the hindrance of diffusive transport in the biofilm and changes in the electrode surface that might possibly be caused by fouling with extracellular organic materials. Therefore, subsequent Cu signals measured in the biofilm were increased by a factor of 8.5.

To evaluate whether cell-bound Cu was labile, the SECM was used to measure a solution containing 0.2 mM Cu before and after addition of 0.08 mg cells. A 4 min preconcentration of Cu was employed for both analyses as in our analysis of the biofilms. The dissolved Cu concentration measured in the presence of cells matched that predicted by the Cu adsorption isotherm. This result indicates that cell-bound Cu is not detected by the SECM.

Metal Transport Modeling. A one-dimensional mass transport model (*25*) was used to describe the spatial distribution of Cu in the biofilms. Basic assumptions in the model include the following: (i) homogeneous distribution of biofilm constituents (e.g., cells and EPS) with uniform thickness; (ii) no resistance to solute transport at the biofilm−bulk fluid interface; i.e. metal concentrations in solution immediately adjacent to the biofilm surface were assumed to be identical to those in bulk solution and no stagnant boundary layer exists across which Cu in the bulk phase must diffuse to get to the biofilm; (iii) the initial metal concentration in biofilms (before addition of Cu) was zero; and (iv) negligible advective mass transport of Cu within the biofilm (i.e., diffusion was the sole transport mechanism).

The concentration (C) of Cu at distance x with an instantaneous point mass source (M_0) after time t is given by (*25*)

$$C(x,t) = \frac{M_0}{\phi R_f A} \frac{1}{\sqrt{4\pi D_e t/R_f}} e^{-x^2/(4D_e t/R_f)} \quad (2)$$

where A (m^2) is the planar biofilm surface area and D_e (m^2/s) is the effective diffusion coefficient in the biofilm that is influenced by tortuosity. A reported biofilm/bulk diffusivity ratio (D_e/D_{aq}) of 0.8 was assumed (*26*, *27*), and D_{aq} for cupric ion in aqueous solution is 7.8×10^{-6} cm^2/s (*26*, *27*). Equation 2 was fit to the experimental Cu data by determining best-fit R_f via least-squares error (LSE) analysis using the SOLVER routine in Microsoft Excel.

Results

Copper Sorption to Planktonic Cells and Retardation Factor. Cu sorption isotherms were evaluated using planktonic cells harvested in stationary phase. Cu sorption to biomass obeyed a linear isotherm up to 0.06 mM Cu (Figure S2, Supporting Information), corresponding to 1 mM added Cu. Most of the added Cu (>95%) was sorbed to planktonic bacteria at the experimental cell concentration ($X = 255 \pm 11$ mg COD/L).

The metal−biomass partition coefficient (K_d), reflecting the distribution of metal between biomass and aqueous phase, was calculated to be 67.1 L/g COD. According to Stewart (*26*), typical values of biofilm porosity and initial biofilm cell density are 0.90 and 5 g/L, respectively. We determined the cell density to be 9.3 ± 2.6 g/L based on the measured biomass COD and the conversion factor of 1.42 g COD/g biomass ($C_5H_7O_2N$, MW = 113). The resulting copper retardation factor, R_f, in biofilms using the K_d derived from Cu adsorption to the planktonic cells was 690 ± 190.

Kinetics of Copper Sorption to Biofilms. Compared with fast metal sorption kinetics in planktonic cell cultures (equilibrium obtained within an hour) (*6*), Cu sorption to *E. coli* biofilms did not attain equilibrium within 2.5 h (Figure 1). After 2.5 h exposure, the amount of sorbed Cu to biofilms was 0.18 mmol/g COD, which is significantly less than 0.74 mmol Cu/g COD observed at equilibrium in planktonic cell cultures.

Electrochemical Measurements by SECM. Dissolved copper (Cu^{2+} and electrochemically labile complexes) in the biofilm was detected by anodic stripping voltammetry (Figure 2). After preconcentration of dissolved copper onto the Pt microelectrode for 4 min at −0.7 V, a voltametric measurement was initiated, and the current for copper oxidation ($Cu^0 \rightarrow Cu^{2+} + 2e$) was observed at a potential of approximately 0.1 V. The oxidation current of hydroxymethyl ferrocene, which served as an internal redox indicator, was found at a potential greater than 0.2 V. Impaired diffusion of hydroxymethyl ferrocene to the microelectrode was caused by close proximity of the electrode to the biofilm surface, and the corresponding sharp drop in the oxidation current for ferrocene (> 50% over 25 μm from the biofilm surface)

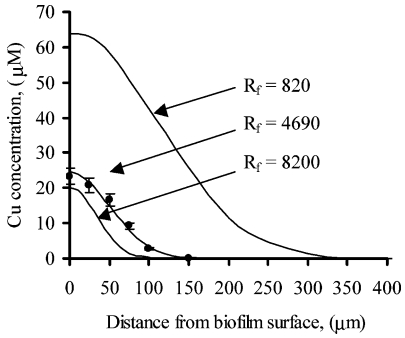

FIGURE 3. Spatial distribution of Cu in an *E. coli* PHL628 biofilm (mass = 2.13 ± 0.46 mg COD) after 2 h exposure to 0.2 mM added Cu (●). A best-fit curve (middle line, retardation factor R_f = 4690 ± 160) to the experimental data was generated from eq 2. Model curve fitting was also done at R_f = 820 or 8200 to evaluate the effect of retardation factor on the Cu distribution in the biofilm. Parameters used follow: t = 2 h, $D_e = 6.2 \times 10^{-6}$ cm²/s. Error bars corresponded to the measured analytical precision of ±9.9% and did not come from replication of the analysis at each point in the profile, because such replication would have impaired with our ability to capture the moving Cu profile.

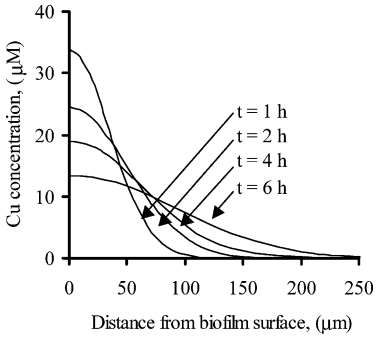

FIGURE 4. Model simulation of the effect of exposure time on the Cu distribution in a biofilm at R_f = 4690.

was used as an operational definition of when the electrode was at the biofilm surface. In a second scan (without the 4 min predeposition of Cu, labeled 3 in Figure 2), no copper oxidation peak was observed. The Cu concentrated on the electrode is released upon oxidation and would result in a transient elevated concentration in the vicinity of the electrode. If these levels were high enough and were not dissipated by Cu adsorption to the biofilm or diffusion away from the biofilm, then they should have been detected without preconcentration. The lack of a Cu reduction ($Cu^{2+} + 2e \rightarrow Cu^0$) peak on the negative scan (labeled 2 in Figure 2) indicates that the oxidized Cu species released from the electrode either diffused away from the vicinity of the electrode tip and/or sorbed to the adjacent biofilm cells. However, the absence of the preconcentration step would reduce the Cu detection limit, and absence of a detectable Cu peak may also reflect diminished analytical sensitivity.

Spatial Distribution of Copper in Biofilms. After biofilm (mass = 2.13 ± 0.46 mg COD, volume-based estimated thickness > 500 μm, and surface area = 4.5×10^{-5} m²) exposure for 2 h to 0.2 mM added Cu, copper was mainly located at the biofilm surface with penetration depth less than 150 μm (Figure 3). The concentration of aqueous Cu species was 23.3 μM at the biofilm/bulk solution interface and decreased to 2.8 μM at the biofilm depth of 100 μm.

Copper Transport Modeling Biofilms. The analytical solution to the diffusion-based model (eq 2) adequately described the spatial distribution of copper in the biofilms (Figure 3). For a boundary condition it was assumed that 70% of added copper sorbed to biofilms after 2 h exposure (based on Figure 1). However, the best fit to the experimental data yielded a retardation factor of 4690 ± 160, more than 6-fold larger than the value (690 ± 190) that was derived from the isotherm for copper adsorption to planktonic cells.

Sensitivity analysis using the model suggests that the retardation factor is the key parameter in determining the spatial distribution of copper. More than 60 μM aqueous Cu species would have accumulated at the biofilm surface with a penetration depth of more than 300 μm if the biofilm had the same retardation capacity as was derived from the planktonic cells (Figure 3). As the R_f value in the model is increased by a factor of 10, both aqueous Cu concentrations at the biofilm surface and penetration depth are calculated to reduce by roughly 3-fold.

For a given initial $[Cu_{total}]$ = 0.56 μmol, the model calculations can be used to illustrate the effect of time on the fate of Cu in the biofilm (Figure 4) and show the expected increasing depth of Cu penetration and the corresponding decrease of the Cu concentration at the biofilm surface.

Discussion

The research reported here allowed us, for the first time, to quantify the Cu concentration gradient in a microbial biofilm. Our results show that after 2 h of exposure copper is mainly located in the test biofilm surface with a penetration depth less than 150 μm (Figure 3). In biofilms, slow penetration of toxic substances, slow growth because of nutrient limitation, and selection for persistent cells with adaptive stress responses are hypothesized to constitute a multifaceted defense (*9*). Knowledge of the spatial distributions of a toxic metal such as Cu provides direct evidence of retarded metal penetration into biofilms. The slow penetration of Cu inside the biofilm structure would act to enhance the survival of cells deep in a biofilm subjected to episodic metal stress.

A mass balance based transport model that accounts for metal sorption and diffusion into biofilms was successful at describing the Cu concentration profile within the biofilm. However, the retardation factor obtained from curve fitting was more than 6-fold larger than that derived from isotherm for Cu adsorption in planktonic cultures of *E. coli* PHL628 (Figure S2, Supporting Information). This difference suggests that it is possible that on a per cell basis within the biofilm there exists an increased level of ligands of EPS origin (e.g., negatively charged sulfhydryl, phosphoryl, and carboxyl groups) that act to increase metal sorption. In addition, the tortuosity factor may be greater than that embodied in the biofilm/bulk diffusivity ratio ($D_e/D_{aq} = 0.8$) assumed for the model calculations. However, using the diffusivity ratio of 0.118 (i.e., $^1/_{8.5}$) that corresponded to our measurement of Cu concentration in the bulk solution and in the biofilm resulted in a bad fit (data not shown). Since coating of the electrode surface may contribute to the change in electrode sensitivity within the biofilm (in addition to a change in the diffusivity of Cu) the ratio of 0.118 is not necessarily expected to reflect the change in the diffusivity ratio. The correction factor used for biofilm Cu concentrations resulted from measurement of Cu in bulk solution and biofilm pore water after multiple exposure of the biofilm to the same Cu concentration. The supposition that the interstitial Cu concentration in the pore water of the biofilm was equal to that of the bulk solution was based on the fact that a discontinuity in Cu concentrations would require that the biofilm have an enormous residual Cu binding capacity available after multiple exposures to the same solution, but was not independently confirmed. The correction factor would change the extent that a discrepancy in Cu concentrations existed, and this change would influence the fitted value for the Cu retardation factor.

Other factors may contribute to larger retardation factors in the biofilms. For example, the overall stability constants

for formation of metal−ligand complexes might be higher within the biofilms as the result of differential gene expression and the production of different EPS components compared to planktonic cultures. A higher local pH in the biofilm might be another important factor contributing to Cu adsorption. Vroom et al. report an average pH of 7.2 ± 0.4 was found in deeper biofilm layers closer to the substratum, relative to a pH of 5.9 ± 0.4 at the biofilm−bulk solution interface (*28*). Finally, as noted above, the model assumption of uniform biofilm thickness and composition was not consistent with the observed heterogeneity of the biofilm (*6*).

In this work, we have extended the application of SECM to microbial biofilms. Since the microelectrode tip senses only the aqueous labile copper species in the biofilms and the concentrations of such species are typically low, dissolved copper must be deposited on the tip at a controlled potential (−0.7 V in this study) and then stripped by scanning the potential anodically (toward a more positive potential) (Figure 2). A preconcentration potential for copper of −0.4 V versus Ag/AgCl was previously applied to measure copper speciation in an ethanol−water mixture (*38*). In our system, we measured aqueous Cu species in the biofilm where Cu concentrations were low and dissociation of labile aqueous Cu complexes (Cu bound to dissolved weak ligands) could be extremely slow. Since the value of the overpotential depends on the "inherent speed" of the electrode reaction, i.e., a slow reaction (with small exchange current density) will require a larger overpotential for a given current density than a fast reaction (with large exchange current density), the relatively large overpotential (−0.7 V) helped us to measure dissolved Cu in the biofilm in a reasonable time. Both the deposition potential and time may be selected to ensure that a suitable signal is obtained. Reduced copper deposited on the tip is oxidized back into solution when the potential reaches the coupled Cu/Cu^{2+} standard potential (0.1 V vs Ag/AgCl as is shown in Figure 2), but a more positive potential (i.e., +0.7 V) was found to be required to completely remove the residual Cu on the microelectrode tip (data not shown) prior to a subsequent measurement.

The value of the steady-state limiting current, $i_{T,\infty}$, for a microdisk electrode embedded in an insulator is given by $i_{T,\infty} = 4nFDCr$, where C is concentration of redox species, n is number of electrons transferred per mole, D is diffusion coefficient of the species, r is the radius of the tip electrode, and F is the Faraday constant (*21*). The resolution of the measurement is therefore largely affected by the radius of the microelectrode and varies with the diffusion coefficient of the species of interest. Aqueous copper concentrations less than 0.2 mM were used to ensure that the mechanism for removal of added Cu was through adsorption to cells and versus precipitation, and were sufficient to discern the spatial resolution of Cu transport into the biofilm.

For diffusive transport of a sorbed compound in a porous medium, the effective diffusion coefficient is divided by the retardation factor (as seen in eq 2). In other words, if the retardation factor is 4960, then the diffusion coefficient is 4960 times smaller than that of a compound that does not sorb to the biofilm. However, the effective diffusion coefficient of a compound that does not react with the biofilm surface is also different from its diffusion coefficient in the bulk solution because of the tortuous diffusion path in the porous biofilm matrix. In the case of an SECM, a change in analytical sensitivity related to fouling of the electrode (if it occurred) could manifest itself in the same way as a reduced diffusion coefficient. An 8.5-fold correction factor for analytical sensitivity was determined (by analysis of the same Cu concentration in the bulk solution and the biofilm pore fluid) and ascribed to the combined effects of tortuosity and change in the electrode surface within the biofilm. The influence of electrode fouling on Cu measurements may change depending on the variable nature of cells and EPS that comprise a biofilm. The correction factor used in this research for Cu measurements within the biofilm should not be assumed to apply to other biofilms without experimental verification.

In many applications, SECM is a noninvasive method, and the microelectrode is not penetrating into the sample matrix. Penetration of the microelectrode into the biofilm could lead to electrode fouling and a change in surface conditions. The reduced surface area of a 2 μm diameter microelectrode in combination with possible fouling blocked our ability to measure low levels of Cu (data not shown), while it was still possible with the larger tip size (25 μm). However, since the Cu concentration profile cannot be measured without inserting the electrode and disturbing the biofilm, there is no clear way to address the magnitude of electrode fouling. The fact that we see a uniform gradient in Cu concentrations within the biofilm establishes that the effect of fouling, if it occurred, was not random. Fouling of the electrode could explain part of the 8.5× difference in its response for the same Cu concentration within the biofilm versus the bulk solution.

The spatial distribution of metals in microbial biofilms has been visualized fluorometrically using multiphoton laser scanning microscopy (*6*) and quantified using scanning electrochemical microscopy in this work. In general, SECM allows measurements of metals at greater depth in biofilms than is amenable to observation with laser scanning microscopy (typically less than 350 μm) with higher sensitivity. However, multiphoton laser scanning microscopy allows direct visualization of metals that would prove difficult for SECM analysis such as zinc because of its large negative standard potential (−0.98 V vs Ag/AgCl for Zn/Zn^{2+}). Nevertheless, multiple metal profiles obtained by SECM could serve as a basis for validation of improved mechanistic-based mass transport models that account for biofilm heterogeneity. Research of this nature would greatly augment our understanding of the function of microbial biofilms under metal stress and their roles as sinks for transient metal spikes in the environment.

Acknowledgments

We appreciate the assistance of Visiting Professor Seong K. Cha. *E. coli* PHL628 was a gift from Dr. Philippe Lajeune. At the time of this work, Z.H. was a postdoctoral fellow with support provided by the Cornell Biocomplexity and Biogeochemistry Initiative.

Supporting Information Available

Schematic of the SECM apparatus (Figure S1) and the Cu adsorption isotherm to planktonic *E. coli* cells (Figure S2). This material is available free of charge via the Internet at http://pubs.acs.org.

Literature Cited

(1) Zobell, C. E.; Allen, E. C. The significance of marine bacteria in the fouling of submerged surfaces. *J. Bacteriol.* **1935**, *29*, 239−251.

(2) Costerton, J. W.; Geesey, G. G.; Cheng, G. K. How bacteria stick. *Sci. Am.* **1978**, *238*, 86−95.

(3) Costerton, J. W.; Lewandowski, Z.; Caldwell, D. E.; Korber, D. R.; Lappin-Scott, H. M. Microbial biofilms. *Ann. Rev. Microbiol.* **1995**, *49*, 711−745.

(4) Davey, M. E.; O'Toole, G. A. Microbial biofilms: from ecology to molecular genetics. *Microbiol. Mol. Biol. Rev.* **2000**, *64*, 847−867.

(5) de Beer, D.; Stoodley, P.; Lewandowski, Z. Effects of biofilm structures on oxygen distribution and mass transport. *Biotechnol. Bioeng.* **1994**, *43*, 1131−1138.

(6) Hu, Z.; Hidalgo, G.; Houston, P. L.; Hay, A. G.; Shuler, M. L.; Abruna, H. D.; Ghiorse, W. C.; Lion, L. W. Determination of

spatial distributions of zinc and active biomass in microbial biofilms by two-photon laser scanning microscopy. *Appl. Environ. Microbiol.* **2005**, *71*, 4014−4021.
(7) Danese, P. N.; Pratt, L. A.; Kolter, R. Exopolysaccharide production is required for development of *Escherichia coli* K-12 biofilm architecture. *J. Bacteriol.* **2000**, *182*, 3593−3596.
(8) Christensen, B. B.; Sternberg, C.; Andersen, J. B.; Eberl, L.; Moller, S.; Givskov, M.; Molin, S. Establishment of new genetic traits in a microbial biofilm community. *Appl. Environ. Microbiol.* **1998**, *64*, 2247−2255.
(9) Mah, T.-F.; Pitts, B.; Pellock, B.; Walker, G. C.; Stewart, P. S.; O'Toole, G. A. A genetic basis for *Pseudomonas aeruginosa* biofilm antibiotic resistance. *Nature* **2003**, *426*, 306−310.
(10) Teitzel, G. M.; Parsek, M. R. Heavy metal resistance of biofilm and planktonic *Pseudomonas aeruginosa*. *Appl. Environ. Microbiol.* **2003**, *69*, 2313−2320.
(11) Lazarova, V.; Manem, J. Biofilm characterization and activity analysis in water and wastewater treatment. *Water Res.* **1995**, *29*, 2227−2245.
(12) Grady, C. P. L., Jr.; Daigger, G. T.; Lim, H. C. *Biological wastewater treatment*; Marcel Dekker: New York, 1999.
(13) Elasri, M. O.; Miller, R. V. Study of the response of a biofilm bacterial community to UV radiation. *Appl. Environ. Microbiol.* **1999**, *65*, 2025−2031.
(14) Ophir, T.; Gutnick, D. A Role for exopolysaccharides in the protection of microorganisms from desiccation. *Appl. Environ. Microbiol.* **1994**, *60*, 740−745.
(15) Nichols, W. W.; Dorrington, S. M.; Slack, M. P. E.; Walmsley, H. L. Inhibition of tobramycin diffusion by binding to alginate. *Antimicrob. Agents Chemother.* **1988**, *32*, 518−523.
(16) Mittelman, M. W.; Geesey, G. G. Copper-binding characteristics of exopolymers from a freshwater-sediment bacterium. *Appl. Environ. Microbiol.* **1985**, *49*, 846−51.
(17) Nelson, Y. M.; Lo, W.; Lion, L. M.; Shuler, M. L.; Ghiorse, W. C. Lead distribution in a simulated aquatic environment - effects of bacterial biofilms and iron-oxide. *Water Res.* **1995**, *29*, 1934−1944.
(18) Beveridge, T. J.; Koval, S. F. Binding of metals to cell envelopes of *Escherichia coli* K-12. *Appl. Environ. Microbiol.* **1981**, *42*, 325−335.
(19) Labrenz, M.; Druschel, G. K.; Thomsen-Ebert, T.; Gilbert, B.; Welch, S. A.; Kemner, K. M.; Logan, G. A.; Summons, R. E.; Stasio, G. D.; Bond, P. L.; Lai, B.; Kelly, S. D.; Banfield, J. F. Formation of sphalerite (ZnS) deposits in natural biofilms of sulfate-reducing bacteria. *Science* **2000**, *290*, 1744−1747.
(20) Bard, A. J.; Fan, F. R. F.; Pierce, D. T.; Unwin, P. R.; Wipf, D. O.; Zhou, F. M. Chemical imaging of surfaces with the scanning electrochemical microscope. *Science* **1991**, *254*, 68−74.
(21) Bard, A. J.; Mirkin, M. V. *Scanning Electrochemical Microscopy*; Marcel Dekker Inc.: New York, 2001.
(22) Vidal, O.; Longin, R.; Prigent-Combaret, C.; Dorel, C.; Hooreman, M.; Lejeune, P. Isolation of an *Escherichia coli* K-12 mutant strain able to form biofilms on inert surfaces: involvement of a new ompR allele that increases curli expression. *J. Bacteriol.* **1998**, *180*, 2442−2449.
(23) APHA, AWWA, and WEF. *Standard methods for the examination of water and wastewater*; Washington, DC, 1998.
(24) Pendley, B. D.; Abruna, H. D. Construction of submicrometer voltammetric electrodes. *Anal. Chem.* **1990**, *62*, 782−784.
(25) Schwartz, F. W.; Zhang, H. *Fundamentals of ground water*; John Wiley & Sons, Inc.: New York, 2002.
(26) Stewart, P. Theoretical aspects of antibiotic diffusion into microbial biofilms. *Antimicrob. Agents Chemother.* **1996**, *40*, 2517−2522.
(27) Quickenden, T. I.; Xu, Q. Toward a reliable value for the diffusion coefficient of cupric ion in aqueous solution. *J. Electrochem. Soc.* **1996**, *143*, 1248−1253.
(28) Vroom, J. M.; De Grauw, K. J.; Gerritsen, H. C.; Bradshaw, D. J.; Marsh, P. D.; Watson, G. K.; Birmingham, J. J.; Allison, C. Depth penetration and detection of pH gradients in biofilms by two-photon excitation microscopy. *Appl. Environ. Microbiol.* **1999**, *65*, 3502−3511.
(29) Zhou, H.; Shiku, H.; Kasai, S.; Noda, H.; Matsue, T.; Ohya-Nishiguchi, H.; Kamada, H. Mapping peroxidase in plant tissues by scanning electrochemical microscopy. *Bioelectrochemistry* **2001**, *54*, 151−156.
(30) Nishizawa, M.; Takoh, K.; Matsue, T. Micropatterning of HeLa cells on glass substrates and evaluation of respiratory activity using microelectrodes. *Langmuir* **2002**, *18*, 3645−3649.
(31) Liu, B.; Cheng, W.; Rotenberg, S. A.; Mirkin, M. V. Scanning electrochemical microscopy of living cells: Part 2. Imaging redox and acid/ basic reactivities. *J. Electroanal. Chem.* **2001**, *500*, 590−597.
(32) Kaya, T.; Torisawa, Y.-s.; Oyamatsu, D.; Nishizawa, M.; Matsue, T. Monitoring the cellular activity of a cultured single cell by scanning electrochemical microscopy (SECM). A comparison with fluorescence viability monitoring. *Biosens. Bioelectron.* **2003**, *18*, 1379−1383.
(33) Gyurcsanyi, R. E.; Jagerszki, G.; Kiss, G.; Toth, K. Chemical imaging of biological systems with the scanning electrochemical microscope. *Bioelectrochemistry* **2004**, *63*, 207−215.
(34) Li, J.; Bishop, P. L. Time course observations of nitrifying biofilm development using microelectrodes. *J. Environ. Eng. Sci.* **2004**, *3*, 523−528.
(35) Okabe, S.; Satoh, H.; Watanabe, Y. In situ analysis of nitrifying biofilms as determined by in situ hybridization and the use of microelectrodes. *Appl. Environ. Microbiol.* **1999**, *65*, 3182−3191.
(36) Satoh, H.; Ono, H.; Rulin, B.; Kamo, J.; Okabe, S.; Fukushi, K. I. Macroscale and microscale analyses of nitrification and denitrification in biofilms attached on membrane aerated biofilm reactors. *Water Res.* **2004**, *38*, 1633−1641.
(37) Werner, E.; Roe, F.; Bugnicourt, A.; Franklin, M. J.; Heydorn, A.; Molin, S.; Pitts, B.; Stewart, P. S. Stratified growth in *Pseudomonas aeruginosa* biofilms. *Appl. Environ. Microbiol.* **2004**, *70*, 6188−6196.
(38) Baldo, M. A.; Daniele, S. Voltammetric monitoring and speciation of copper ions in Italian "Grappa" with platinum microelectrodes. *Electroanalysis* **2006**, *18*, 633−639.

Received for review May 30, 2006. Revised manuscript received October 31, 2006. Accepted November 2, 2006.

ES061293K